The Application of Mesoturbulence to Stellar Atmospheres

E. Sedlmayr
Institut für Theoretische Astrophysik
der Universität Heidelberg
Heidelberg, FRG

Abstract

For realistic stellar atmospheres the equations describing mesoturbulent
line formation are solved numerically. The general dependence of theo-
retical line profiles and equivalent widths on the correlation length l
and the mean square turbulent velocity σ is demonstrated. Also empiri-
cal relations between the basic parameters of the micro-macroturbulence
description (v_{mic}, v_{mac}) and the fundamental mesoturbulence parameters
(l, σ) are derived.

Introduction

It has been shown (see Traving's contribution) that turbulence in
stellar atmospheres is necessarily of finite scale length. So meso-
turbulence is a very common phenomenon which should be taken into
account in line formation studies.

In this contribution we shall apply the mesoturbulence formalism
(e.g. Auvergne et al. (1973), Gail et al. (1974), Gail and Sedlmayr
(1974), Frisch (1975)) to line formation in realistic atmospheres.
Our aimes are

(i)   to demonstrate the basic effects of the correlation length l
      and the mean square turbulent velocity σ on the line profiles
      and equivalent widths, and

(ii) to derive empirical relations between the classical parameters
      (microturbulent velocity v_{mic} and macroturbulent velocity v_{mac})
      and the fundamental parameters of the mesoturbulence description
      l and σ.

1. The Numerical Method

Two particular stochastic models have been adopted for discussing
mesoturbulent line formation in stellar atmospheres:

a) The Uhlenbeck-Ornstein Process (UOP)

The UOP is a stationary Markovian process continuous in space with
both Gaussian one-point and two-point velocity distribution functions.
The resulting transfer equation for the monochromatic local condition-
al intensity q(s,v) is therefore a parabolic partial differential
equation of Fokker-Planck type (Gail et al. (1974), Gail and
Sedlmayr (1974)):

$$\frac{\partial q}{\partial s} = \frac{1}{l} \left(-v \frac{\partial q}{\partial v} + \sigma^2 \frac{\partial^2 q}{\partial v^2}\right) - (\kappa_o \phi + \kappa_c)(q - S), \tag{1}$$

with s being the distance along the ray, v the actual velocity, $\kappa_o \phi$
and κ_c the line and continuum absorption coefficients. $\phi(s,v,\sigma,\Delta\lambda)$ is
the profile function and S the monochromatic local source function.
κ_o, κ_c and S are assumed to be independent of the velocity v.

The expectation value for the monochromatic local intensity $<I(s)>$
is obtained by multiplication of q by the one-point velocity distri-
bution $\mathbb{P}_1(v)$ and integration with respect to the velocity variable:

$$<I(s)> = \int_{-\infty}^{+\infty} dv \, \mathbb{P}_1(v) q(s,v). \tag{2}$$

Given a model atmosphere which provides κ_o, κ_c and S, and given
appropriate initial and boundary conditions the above transfer
equation can be solved numerically straight-forward by the Crank-
Nicholson method (e.g. Richtmyer and Morton,(1967)).

Without going into any technical details I shall point to the only
problem which may arise and which results from an inconsistent in-
corporation of the boundary conditions: The natural boundary condi-
tions for our problem are given by the asymptotic limits $v \to \pm\infty$,
where the line absorption vanishes and the radiative transfer is con-
trolled by continuous absorption only. It turns out that in the case
of strong lines or large turbulent velocities one has to take into
account rather large $|v|$ to approach these limits with sufficient
accuracy and to avoid slight instabilities near the boundaries.

b) The Kubo-Anderson Process (KAP)

The KAP is a stationary Markovian process discontinuous in space with
a Gaussian one-point velocity distribution function (like UOP) but a
non-Gaussian two-point velocity distribution function which bridges
the gap between the two limiting cases of complete correlation and
complete noncorrelation by a linear ansatz (Auvergne et al. (1973),
Frisch and Frisch (1975); see also Traving's contribution).

Using the KAP one arrives at an integro-differential equation for the
monochromatic local conditional intensity $q(s,v)$:

$$\frac{\partial q(s,v)}{\partial s} = \frac{1}{l}\left\{ \int_{-\infty}^{+\infty} dv' \mathbb{P}_1(v')q(s,v') - q(s,v)\right\} - (\kappa_o \phi + \kappa_c)(q(s,v)-S). \tag{3}$$

From this equation the expectation value of the emergent intensity can
be calculated

(i)   by means of the semianalytical methods used by Auvergne et al.
      (1973), and Frisch (1975) or

(ii) by a direct numerical solution of (3) and a subsequent integration
      according to (2). A proper discretisation in the velocity coordi-
      nate reduces this equation to a system of coupled linear ordinary
      differential equations which can be solved by standard methods
      (Gail et al. (1976).

However, both procedures have inherent specific difficulties either
connected with instabilities in the region of very small l (microtur-
bulent limit) or problems of large matrix size respectively.

Thus for numerical reasons we consider the straigthforward solution
of the Fokker-Planck equation described in a) to be more efficient.

2. Effect of a Correlated Velocity Field on Line Profiles and Equivalent Widths

Adopting the UOP line profiles, equivalent widths and curves of
growth have been calculated for selected lines of particular elements
formed in the solar photosphere. In order to account for the effects of
model atmospheres different from the sun we have extended these com-
putations to atmospheres of earlier and later spectral type (AOV (Wega)
and K2III (Arcturus)) also.

All calculated profiles show a similar monotonic dependence on l and σ
respectively. Thus for demonstration of principle effects we may re-
strict ourselves to the discussion of an arbitrary line in the solar
photosphere.

For a given mean square turbulent velocity σ and a non-negative corre-
lation function microturbulence always yields the maximum absorption
for a spectral line. Hence line profiles which originate in a velocity
field determined by a small scale length are always deeper than the
corresponding profiles formed in a velocity field with equal turbulent
velocity but larger correlation length.

This is clearly seen in Fig. 1a, where for the line FeI λ62oo theore-
tical profiles are plotted for σ = 2 km/s and different values for the
correlation length l. l = 1 km and l = 10^4 km refer to the microturbu-
lent and macroturbulent limit respectively.

If the correlation of the velocity field is increased for fixed σ both
the line depth and the width of the corresponding profiles decrease
monotonically until for very large l ($\gtrsim$ 3ooo km) saturation is achiev-
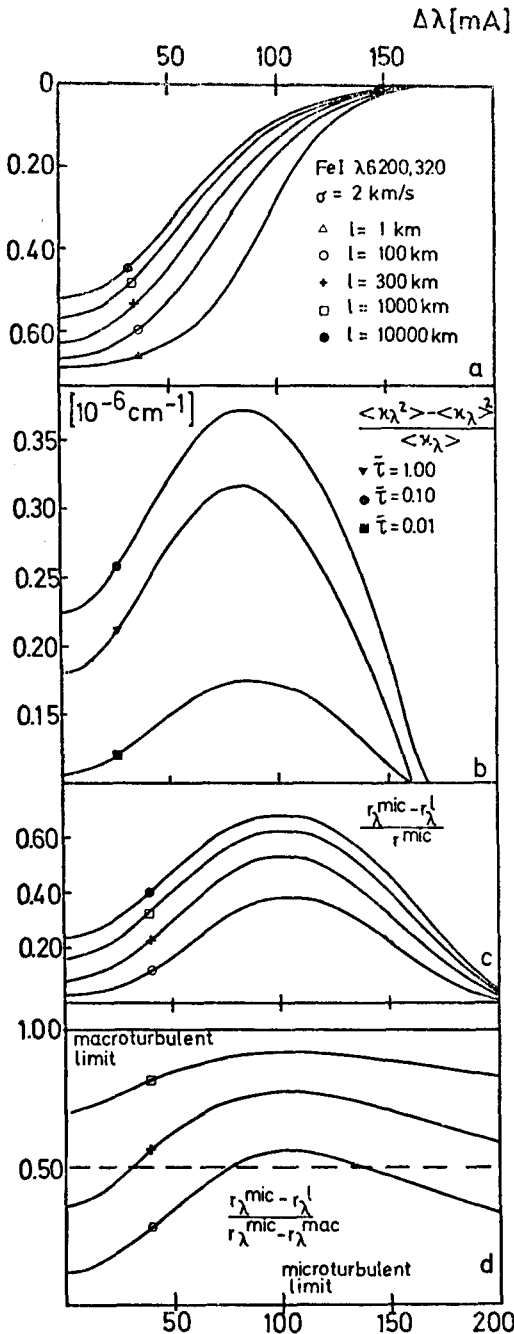ed (macroturbulent limit).

This general behaviour is also demonstrated in Fig. 2 which for differ-
ent values of σ - but for the same line - shows the effect of the
correlation length l on the central depth r_o and the equivalent width
W_λ of the emergent profile.

For σ $\leq$ 1 km/s thermal broadening exerts the essential influence on
the absorption coefficient. Hence for small mean square turbulent
velocities both the central depths and equivalent widths depend only
slightly on l. With increasing σ the thermal contribution becomes more
and more negligible and the influence of the correlation of the turbu-
lence field on r_o and W_λ is considerably increased.

For large σ both r_o and W_λ become monotonically strongly decreasing
functions with increasing l approaching their minimum value in the
macroturbulent limit. In this case the equivalent widths become inde-
pendent on σ; a fact which causes all W_λ - curves in Fig. 2 to converge
asymptotically.

The theory of mesoturbulent line formation provides a simple criterion
which allows a quantitative estimate of a profile's deviation from the
corresponding microturbulent result (see Traving's contribution). Accord-
ing to this criterion microturbulence should be a good approximation if

Fig. 1: All calculations have been performed on the basis of the empirical solar model atmosphere of Holweger (1967) assuming a mean square turbulent velocity σ = 2 km/s and a normal iron abundance.

$\Delta\lambda[mA]$

FeI λ6200,320
σ = 2 km/s

△ l = 1 km
○ l = 100 km
+ l = 300 km
□ l = 1000 km
● l = 10000 km

a

$[10^{-6} cm^{-1}]$

$\frac{<\kappa_\lambda^2>-<\kappa_\lambda>^2}{<\kappa_\lambda>}$

▼ τ̄ = 1.00
● τ̄ = 0.10
■ τ̄ = 0.01

b

$\frac{r_\lambda^{mic}-r_\lambda^l}{r_\lambda^{mic}}$

c

macroturbulent
limit

$\frac{r_\lambda^{mic}-r_\lambda^l}{r_\lambda^{mic}-r_\lambda^{mac}}$

microturbulent
limit

d

a) Theoretical profiles of the line FeI λ62oo for different values of the correlation length l. l ≤ 1 km and l ≥ 3ooo km correspond to the micro- and macroturbulent limit respectively.

b) Mean square root of the line absorption coefficient
$\kappa_\lambda = \kappa_o(s)\phi(s,v,\sigma,\Delta\lambda)$ versus λ at different optical depths (Rosseland depth scale).

c) Deviation of a profile (calculated with a finite correlation length) from the microturbulent profile normated to the microturbulent value.

d) Deviation of a profile (calculated with a finite correlation length) from the microturbulent profile normated to the difference between the micro- and macroturbulent profile. This quantity indicates quantitatively which part of a profile is mainly determined by microturbulent or macroturbulent conditions respectively.
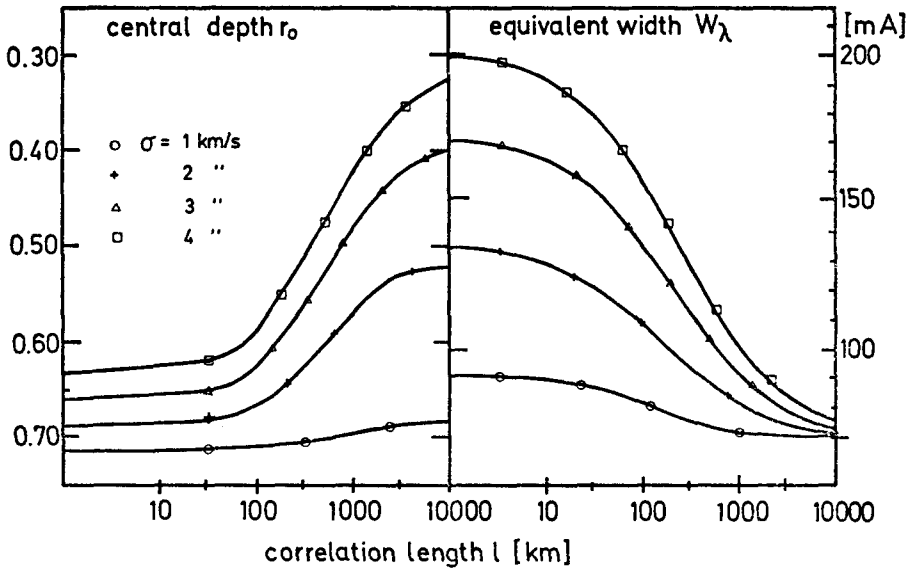
Fig. 2: Dependence of the central depth r_0 and the equivalent width W_λ of the line FeI $\lambda 6200$ on the correlation length l for different values of the mean square turbulent velocity σ.

the condition

$$\frac{1}{2} \, \tau_1 \cdot \tau_s \frac{<\kappa^2> - <\kappa>^2}{<\kappa>^2} << 1 \tag{4}$$

holds. $<...>$ indicates the average values calculated by means of the one-point velocity distribution function, and $\tau_1 = l<\kappa>$ and $\tau_s = s<\kappa>$ are characteristic optical depths corresponding to the correlation length and the relevant geometrical depth of line formation respectively. Thus by definition τ_s is usually of the order of unity. With $\tau_s = 1$ and $\tau_1 = l<\kappa>$ the proper wavelength dependence of (4) is essentially given by the quantity $(<\kappa^2> - <\kappa>^2)/<\kappa>$, which is plotted in Fig. 1b for relevant optical depths $\bar{\tau}$.

From Fig. 1b we expect the largest deviations for a line profile calculated with fixed values l,σ from the corresponding microturbulent result to occur at the transition from the core to the wing of the line where the curves $(<\kappa^2> - <\kappa>^2)/<\kappa>$ show a pronounced maximum.

However, condition (4) is primarily a mathematical condition which for each wavelength measures the magnitude of the difference between a profile calculated with finite correlation length and the same profile

calculated under the assumption of microturbulence. Obviously Fig. 1b
shows that for the line centre and the outer wings the deviations from
the microturbulent profile are considerably smaller than for the
transition region even for large l. This is confirmed by the results
in Fig. 1c where for different values of l the normated deviations
from the microturbulent profile are plotted versus λ. However, this
does not indicate that for large l these parts of the line do form
under microturbulent conditions, but only that for these parts of the
profile the microturbulent result is a reliable approximation for the
true profile.

In order to decide whether micro- or macroturbulent conditions pre-
vail we have plotted in Fig. 1d the quantity

$$d_\lambda^{l,\sigma} = (r_\lambda^{mic,\sigma} - r_\lambda^{l,\sigma})/(r_\lambda^{mic,\sigma} - r_\lambda^{mac,\sigma}) \tag{5}$$

for $\sigma = 2$ km/s and several values of l. Essentially two regions can be
distinguished:

1) $o \lesssim d_\lambda^{l,\sigma} \lesssim \frac{1}{2}$: Microturbulence governs the radiative transfer. For
   $l \simeq 1oo...5oo$ km this case applies only to the line cores and the
   outer wings. We infer that for smaller l the entire line is formed
   under microturbulent conditions.

2) $\frac{1}{2} \lesssim d_\lambda^{l,\sigma} \lesssim 1$: Macroturbulence governs the radiative transfer. This
   effect is most pronounced at those parts of the profile where the
   curves of Fig. 1b have their maximum. For correlation lengths
   $l \gtrsim 1ooo$ km the entire line is formed under macroturbulent condi-
   tions.

Throughout this discussion the UOP has been adopted. Using the KAP
would yield quantitatively very similar results. However, due to the
underlying cell structure of this model, KAP results always show a
higher degree of correlation than the corresponding UOP results ob-
tained for the same line with an identical correlation length and mean
square turbulent velocity, (Frisch (1975), Gail et al. (1976)).

3. Empirical Relations between (v_{mic}, v_{mac}) and (l,σ)

In this section we want to present preliminary results obtained by a
cooperation with H. Holweger (Kiel).

There are essentially two reasons which provide the motivation for the

study of the relations between the classical micro-macroturbulence
parameters (v_{mic}, v_{mac}) and the fundamental parameters of the mesotur-
bulence description (l,σ).

1) In classical theory v_{mic} and v_{mac} have been introduced as free para-
meters to fit observed and calculated profiles and curves of growth. If
it is possible to relate these quantities in a simple way to l and σ
the corresponding parameters of the turbulent velocity field, we
arrive at a physically more justified interpretation of v_{mic} and v_{mac}.

2) In the past analyses of stellar atmospheres on the basis of classi-
cal micro- macroturbulence theory have been performed providing em-
pirical values for v_{mic} and v_{mac}. By means of relations between
these quantities and l and σ one is in the position to determine the
mean turbulent velocity and the correlation length of the turbulence
field for such atmospheres without reanalizing them by means of the
more complex mesoturbulence formalism.

In order to find out the relations between these two sets of parameters
the following procedure has been used:

For a given model atmosphere and artificial data for FeI- and FeII-
lines curve of growth have been computed for a l- σ- grid. On the other
hand the conventional microturbulence approach has been used to cal-
culate an independent set of curves of growth for the same transitions.
By varying the parameter v_{mic} an optimum fit between these two sets of
data has been found using as criterion the minimum value of

$$\phi = \Sigma_{lines} \left[(w_\lambda^{mic} - w_\lambda^{l,\sigma})/w_\lambda^{l,\sigma} \right]^2 \quad . \tag{6}$$

Having thus determined a relation between v_{mic} and l,σ we use
the calculated profiles $r_{\Delta\lambda}^{mic,mac}$ and $r_{\Delta\lambda}^{l,\sigma}$ to derive an optimum macro-
turbulent velocity v_{mac} by minimizing

$$\psi = \Sigma_{lines} \Sigma_{\Delta\lambda_j} (r_{\Delta\lambda_j}^{mic,mac} - r_{\Delta\lambda_j}^{l,\sigma})^2 \quad . \tag{7}$$

In this way for each pair (l,σ) a corresponding pair (v_{mic}, v_{mac}) has
been determined empirically.

A typical result for the sun is shown in Fig. 3 where for three differ-
ent artificial iron lines the optimum values for v_{mic} and v_{mac} are
plotted versus l for a given mean square turbulent velocity σ. We see
the expected strong correlation between the "decrease" of microturbu-
lence and the corresponding "increase" of macroturbulence with growing
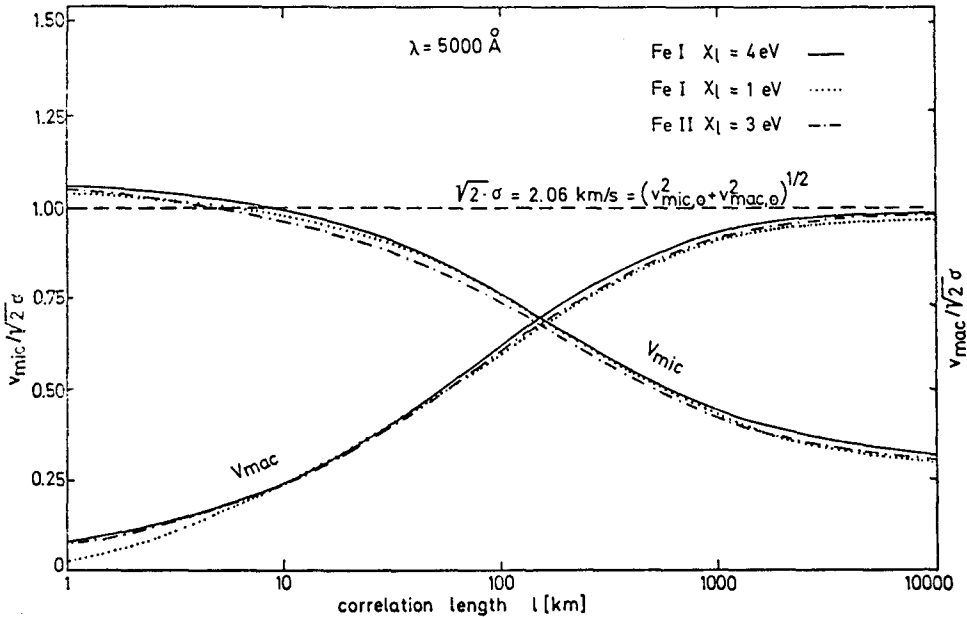
correlation of the turbulence field.

Fig. 3: Empirical dependence of the classical micro- and macroturbulent velocity on the correlation length l, derived on the basis of three artificial iron lines with wavelength $\lambda = 5000$ A and an excitation energy of the lower level χ_l. (A mean square turbulent velocity $\sqrt{2}\sigma = 2.06$ km/s has been chosen, because this value - according to relation (8) - corresponds exactly to the empirical values $v_{mic,\odot} = 1$ km/s and $v_{mac,\odot} = 1.8$ km/s. (Empirical model photosphere of Holweger (1967)).

The curves of Fig. 3 resemble to some extent the filter functions introduced by de Jager (1972, 1979), de Jager and Vermue (1977) and Vermue and de Jager (1979) in order to describe the fraction of energy contained in the microturbulent and macroturbulent mode respectively. However, there are significant conceptual differences:

(i) In the description of de Jager and Vermue the adopted definition of microturbulence is based solely on the investigation of weak lines, whereas in our approach the microturbulence velocity is derived by a classical curve of growth analysis with no restriction concerning the line strength.

(ii) The filter function method is based on the consideration of one single mode u(k) of the Fourier spectrum of the turbulent field, whereas our statistical approach by means of probability distributions and correlation functions describes the mean values of the

turbulent field to which all modes contribute.

The fact, that in the filter function presentation the transition from the micro- to the macroturbulent regime is much steeper than in our approach may be due to this difference.

In order to demonstrate the empirical relations between (v_{mic}, v_{mac}) and $(1, \sigma)$ more clearly for an arbitrary line of the solar photosphere the quantity $(v^2_{mic} + v^2_{mac})^{1/2}$ is plotted in Fig. 4a versus 1 for a given σ. This plot provides strong evidence for a relation of the form

$$2\sigma^2 = v^2_{mic} + v^2_{mac} \tag{8}$$

which seems to hold with considerable accuracy at least within the region of relevant 1 values.

This relation, which has been confirmed by computing a large number of lines, also holds for different stellar atmospheres (AOV, K2III). In no case deviations from the relation (8) of more than few percents have been found.
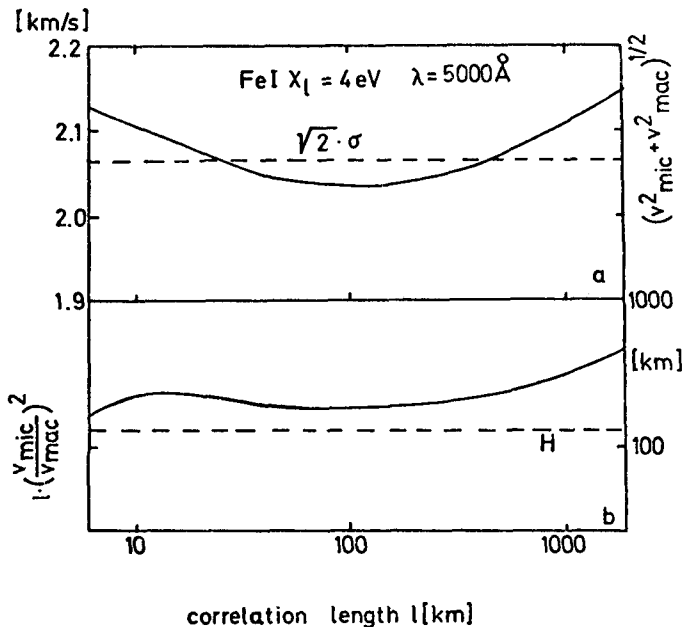

Fig. 4: The quantities $(v^2_{mic} + v^2_{mac})^{1/2}$ and $1(\frac{v_{mic}}{v_{mac}})^2$ versus λ for the same line as Fig. 3. H is the pressure scale height at the depth of line formation.

To relate the correlation length l to the velocity parameters an
additional typical scale length H characterizing the atmosphere has to
be introduced. This scale length turns out to be the pressure scale
height taken at an optical depth which corresponds to the region of
line formation. From Fig. 4b, where the quantity $l(\frac{v_{mic}}{v_{mac}})^2$ is plotted
versus l, we conclude that for l values which can be determined reliab-
ly a satisfactory fit is obtained by the relation

$$\frac{H}{l} \simeq (\frac{v_{mic}}{v_{mac}})^2 \quad . \tag{9}$$

Relation (9), like (8), has been confirmed for the considered atmo-
spheres by calculating a large number of lines. In no case a deviation
of more than 1o percent has been found.

Such empirical relations should reflect similar relations connecting
the basic physics of these approaches. In order to give an at least
heuristic explanation for these basic relations we require that the
corresponding one-point and two-point velocity distribution functions
describing classical micro-macroturbulence and mesoturbulence respect-
ively are identical:

$$\mathbb{P}_1^{mic,mac}(v) \equiv \mathbb{P}_1^{l,\sigma}(v) \tag{1o}$$

and

$$\mathbb{P}_2^{mic,mac}(v_1,v_2) \equiv \mathbb{P}_2^{l,\sigma}(v_1,v_2,\rho) \quad . \tag{11}$$

With

$$\mathbb{P}_1^{mic,mac}(v) = \left[\pi(v_{mic}^2 + v_{mac}^2)\right]^{-1/2} \exp\left[-\frac{v^2}{v_{mic}^2 + v_{mac}^2}\right] \tag{12}$$

and

$$\mathbb{P}_1^{l,\sigma}(v) = \left[\pi 2\sigma\right]^{-1/2} \exp\left[-\frac{v^2}{2\sigma^2}\right] \tag{13}$$

one immediately obtains relation

$$(8) \quad 2\sigma^2 = v_{mic}^2 + v_{mac}^2 \quad .$$

From

$$\mathbb{P}_2^{mic,mac}(v_1,v_2) = \left[\pi^2 v_{mic}^2 (v_{mic}^2 + 2v_{mac}^2)\right]^{-1/2} , \tag{14}$$

$$\exp\left[-\frac{(v_{mic}^2 + v_{mac}^2)(v_1^2 + v_2^2) - 2v_{mac}^2 v_1 v_2}{v_{mic}^2(v_{mic}^2 + 2v_{mac}^2)}\right]$$

and

$$\mathbb{P}_2^{1,\sigma}(v_1,v_2,\rho) = \left[\pi 2\sigma^2(1-\rho^2)^{1/2}\right]^{-1} \exp\left[-\frac{v_1^2 + v_2^2 - 2\rho v_1 v_2}{2\sigma^2(1-\rho^2)}\right] \tag{15}$$

with

$$\rho(s) = \exp(-\frac{s}{l}) . \tag{16}$$

One sees that eq. (11) can hold only for one particular value of the correlation function $\rho(s)$.

Using eq. (8) one obtains for this particular value

$$\rho(s) = \frac{v_{mac}^2}{v_{mic}^2 + v_{mac}^2} \tag{17}$$

which for $s << l$ immediately yields the approximate relation

$$\frac{s}{l} \simeq (\frac{v_{mic}}{v_{mac}})^2 . \tag{18}$$

So at least the analytical form of the empirical result (9) is recovered. As s is a typical geometrical dimension of the line forming region, it should be closely connected with the scale height H introduced in (9).

In order to justify the assumption $s << l$ we plot in Fig. 3 two horizontal lines indicating the empirically determined values for $v_{mic,\odot}$ and $v_{mac,\odot}$ respectively (Holweger (1967)). This plot is shown in Fig. 3a. The abscissas of the intersection points of each line with the corresponding v_{mic}- or v_{mac}- curves determine the region of best fitting l values. We see that the optimum l values are confined to a rather narrow interval of 53o km $\leq$ l $\leq$ 64o km. These l values are considerably larger than the scale height H shown in Fig. 4b, which justifies our above assumption.
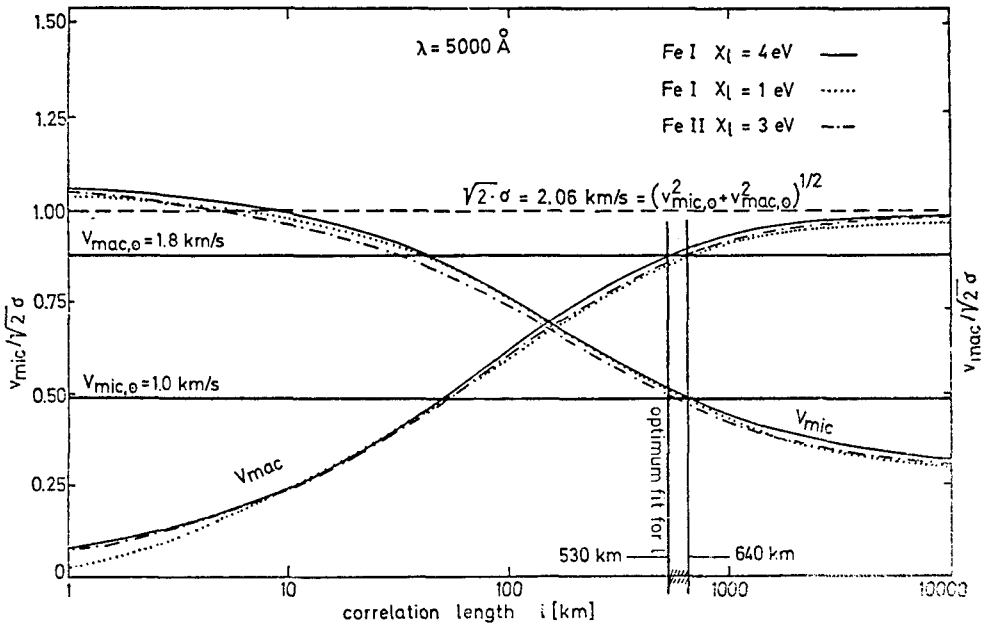
Fig. 3a: See Fig. 3. The horizontal lines indicate the empirically determined photospheric values for $v_{mic,\odot}$ and $v_{mac,\odot}$ (Holweger (1967)). The vertical lines determine the interval of best fitting l values (strongly crosshatched on the abcissa).

Our result for the optimum correlation of $l \simeq 600$ km for the solar photosphere is in close agreement with the average value $\frac{2\pi}{k} \simeq 600$ km for the inverse wavenumber of the velocity spectrum derived by de Jager and Vermue (1977) by means of the filter function method. The fact that these very different methods yield approximately the same results provides confidence for this value of the scale length.

Conclusion

Our analysis of the radiative transfer of selected lines in three particular atmospheres (AOV (Wega), G2V (Sun), K2III (Arcturus)) demonstrates that a finite correlation length of the turbulent velocity field exerts a strong influence on the line formation. The general dependence of this effect on the basic parameters (l,σ) is similar in all atmospheres and for all profiles considered.

A comparison between profiles and curves of growth computed by means of the mesoturbulence formalism at one hand and by the classical micro-

macroturbulence method at the other, provides strong evidence for very close relations between $(1,\sigma)$ and (v_{mic}, v_{mac}). These relations allow a reinterpretation of the classical micro-macroturbulence dichotomy which is closer to physics.

References

Auvergne, M.; Frisch, H.; Frisch, U.; Froeschlé, Ch.; Pouquet, A.;1973, Astron. & Astrophys. $\underline{29}$, 93

Brissaud, A.; Frisch, U.; 1974, J. Math. Phys., $\underline{15}$, 524

De Jager, C.; 1972, Solar Phys. $\underline{25}$, 71

De Jager, C.; 1978, Astrophys. Space Sci. $\underline{59}$, 165

De Jager, C.; Vermue, J.; 1977, Solar Phys. $\underline{54}$, 313

Frisch, U.; 1968, in Probabilistic Methods in Applied Mathematics, edited by A.T. Bharucha-Reid, Academic Press, New York and London

Frisch, H.; Frisch, U., 1976 in Physique des mouvements dans les atmosphères stellaires, Colloques internationaux du centre national de la recherche scientifique, Paris p.113

Frisch, H.; Frisch, U., 1976, Monthly Notices Roy.Astron. Soc. $\underline{175}$, 157

Gail, H.-P.; Hundt, F.; Kegel, W.H.; Schmid-Burgk, J.; Traving, G., 1974, Astron. & Astrophys. $\underline{32}$, 65

Gail, H.-P.; Sedlmayr, E., 1974, Astron. & Astrophys. $\underline{36}$, 17

Gail, H.-P.; Kegel, W.H.; Sedlmayr, E., 1975, Astron. & Astrophys.$\underline{42}$,81

Gail, H.-P.; Sedlmayr, E.; Traving, G., 1975, Astron. & Astrophys.$\underline{44}$,421

Gail, H.-P.; Sedlmayr, E.; Traving, G., 1976, Astron. & Astrophys.$\underline{46}$,441

Gail, H.-P.; Sedlmayr, E.; Traving, G., 1979, JQSRT, in press

Gray, D.F., 1977, Astrophys. J. $\underline{218}$, 53o

Gray, D.F., 1978, Solar Phys. $\underline{59}$, 193

Hearn, A.G., 1974, Astron. & Astrophys. $\underline{31}$, 415

Holweger, H., 1967, Z. Astrophys. $\underline{65}$, 365

Hundt, E., 1973, Astron. & Astrophys. $\underline{29}$, 17

Magnan, C., 1976, JQSRT $\underline{16}$, 281

Magnan, C., 1976, in Physique des mouvements dans les atmosphères
             stellaires, Colloque internationaux du CNRS, Paris p. 179

Rybicki, G., 1976, in Physique des mouvements dans les atmosphères
             stellaires, Colloque internationaux du CNRS, Paris p. 189

Schmid-Burgk, J., 1974, Astron. & Astrophys. 32, 73

Sedlmayr, E., 1976, in Physique des mouvements dans les atmosphères
             stellaires, Colloque internationaux du CNRS, Paris p. 157

Struve, O.; Elvey, C.T., 1934, Astrophys. J. 79, 4o9

Traving, G., 1964, Z. Astrophys. 6o, 167

Traving, G., 1975, in Problems in Stellar Atmospheres and Envelopes
             eds. B. Baschek, W.H. Kegel and G. Traving, Springer-
             Verlag, Berlin-Heidelberg-New York p. 325

Traving, G., 1976, in Physique des mouvements dans les atmosphères
             stellaires, Colloques internationaux du CNRS, Paris p. 145

Vermue, J.; de Jager, C., 1979, Astrophys. Space Sci. 61, 129

Wang, M.CH.; Uhlenbeck, G.E., 1945, Rev. Mod. Phys. 17, 323